

AD-A116 503

MASSACHUSETTS INST OF TECH LEXINGTON LINCOLN LAB F/G 9/5
INTERFERENCE SOURCES AND DEGREES OF FREEDOM IN ADAPTIVE NULLING--ETC(U)
MAY 82 A J FENN F19628-80-C-0002

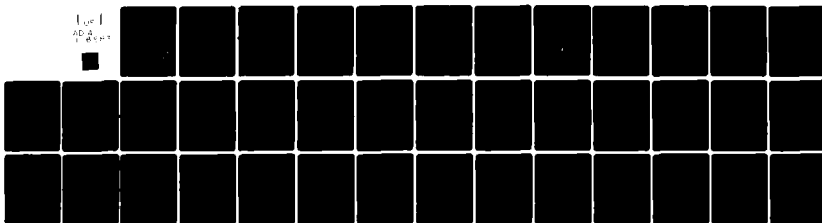
UNCLASSIFIED

TR-604

ESD-TR-82-047

NL

1 of 1
AD-A
1-80-1



END
DATE
FILMED
7-82
DTIC

AD A116583

ESD-TR-82-047

1.2

Technical Report

604

Interference Sources and Degrees of Freedom in Adaptive Nulling Antennas

A.J. Fenn

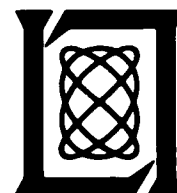
12 May 1982

Prepared for the Defense Communications Agency
under Electronic Systems Division Contract F19628-80-C-0002 by

Lincoln Laboratory

MASSACHUSETTS INSTITUTE OF TECHNOLOGY

LEXINGTON, MASSACHUSETTS



Approved for public release; distribution unlimited.

DTIC FILE COPY

82 07 07 A
003

The work reported in this document was performed at Lincoln Laboratory, a center for research operated by Massachusetts Institute of Technology. This work was sponsored by the Military Satellite Communications Systems Office of the Defense Communications Agency under Air Force Contract F19628-80-C-0002.

This report may be reproduced to satisfy needs of U.S. Government agencies.

The views and conclusions contained in this document are those of the contractor and should not be interpreted as necessarily representing the official policies, either expressed or implied, of the United States Government.

The Public Affairs Office has reviewed this report, and it is releasable to the National Technical Information Service, where it will be available to the general public, including foreign nationals.

This technical report has been reviewed and is approved for publication.

FOR THE COMMANDER

Raymond L. Loiselle

Raymond L. Loiselle, Lt.Col., USAF
Chief, ESD Lincoln Laboratory Project Office

Non-Lincoln Recipients

PLEASE DO NOT RETURN

Permission is given to destroy this document
when it is no longer needed.

MASSACHUSETTS INSTITUTE OF TECHNOLOGY
LINCOLN LABORATORY

**INTERFERENCE SOURCES AND DEGREES OF FREEDOM
IN ADAPTIVE NULLING ANTENNAS**

A.J. FENN

Group 61

TECHNICAL REPORT 604

12 MAY 1982

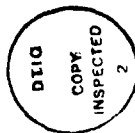
Approved for public release; distribution unlimited.

LEXINGTON

MASSACHUSETTS

ABSTRACT

It is sometimes desirable to know how many interference sources an N -element phased array or N -beam multiple-beam antenna can adaptively null. This problem is usually addressed by considering the antenna to have at most $N-1$ degrees of freedom available for placing nulls on interference sources. However, if some of the $N-1$ sources are very close together, it is possible that less than $N-1$ degrees of freedom are used. This paper quantitatively describes this effect by examining the eigenvalue spread of the interference covariance matrix. It is shown in the case of two equal-power interference sources in the field of view of either a multiple-beam antenna, or a phased array antenna, the two dominant eigenvalues are approximately equal when the source separation is equal to one half-power beamwidth. In other words, two degrees of freedom are consumed by two interference sources when they are separated by approximately one half-power beamwidth. This effect is also investigated for several configurations of three interference sources. To consume three degrees of freedom, it is shown that the eigenvalue spread is dependent on the interference source configuration and the antenna geometry.



A

TABLE OF CONTENTS

Abstract	iii
List of Illustrations	vi
I. Introduction	1
A. Consumption of Adaptive Antenna Degrees of Freedom	1
II. Formulation	12
A. Applebaum-Howells Analog Servo-Control-Loop Processor	12
B. Eigenvalues and Eigenvectors of the Interference Covariance Matrix	13
III. Two Interference Sources	16
A. Multiple-Beam Antenna	16
B. Phased Array Antenna	19
IV. Three Interference Sources	23
A. MBA and Phased Array	23
V. Discussion and Conclusions	26
Appendix A - Derivation of the Applebaum-Howells Steady State Adapted Weight Equation in Eigenspace	28
References	34
Acknowledgments	34

ILLUSTRATIONS

Figure No.

- | | |
|---|----|
| 1. Geometry for two interference sources (I_1, I_2) in the field of view of either a multiple-beam antenna or a phased array antenna. | 2 |
| 2. Block diagram for an N-channel adaptive nulling system. | 4 |
| 3. Radiation pattern before adaption. | 5 |
| 4. Radiation pattern using the dominant eigenvector as a weight. | 6 |
| 5. Radiation pattern after adaption. | 8 |
| 6. Typical null-region shape for a communications link where the user is in a known location. | 9 |
| 7. Typical null-region shapes for various interference source spacings for a communications link where the users are in unknown locations. | 10 |
| 8. Hexagonal beam positions for a 19-beam MBA. | 17 |
| 9. Eigenvalue spread as a function of the separation between two interference sources in the field of view of a 19-beam MBA. | 18 |
| 10. A ten-element circular ring array designed for a 2° coverage area. | 20 |
| 11. Eigenvalue spread as a function of the separation between two interference sources in the field of view of a ten-element circular ring array. | 22 |

I. INTRODUCTION

The goal of this paper is to provide a basic understanding of how the degrees of freedom of an adaptive nulling antenna are consumed by undesired interference signals. This problem is usually addressed by associating the number of interference sources which are nulled with the number of degrees of freedom that are consumed. This approach is generally not satisfactory because the number of degrees of freedom consumed depends on the interference source spacing and the antenna geometry. A better method is to compute the eigenvalues of the interference covariance matrix and examine their amplitude spread^[1] as a function of the source spacing; the case of two sources (I_1 , I_2) is shown in Figure 1. This is demonstrated for both a multiple beam antenna (MBA) and a phased array antenna. The Applebaum-Howells analog servo-control-loop processor is used as the adaptive nulling algorithm. However, the results are expected to be fundamental to the performance of any adaptive antenna.

A. Consumption of Adaptive Antenna Degrees of Freedom

A measure of the susceptibility to interference for an adaptive antenna is the spread of the eigenvalues of the covariance matrix formed by the cross-correlation of interference signals received at each antenna port. The spatial location and strength of the interference source (or sources) affects the eigenvalues and the interference-to-receiver noise ratio prior to adaption. The quiescent (before adaption) radiation pattern of the adaptive antenna determines the initial value of the interference-to-receiver noise ratio. However, the eigenvalues depend only on the radiation pattern and

117378-N

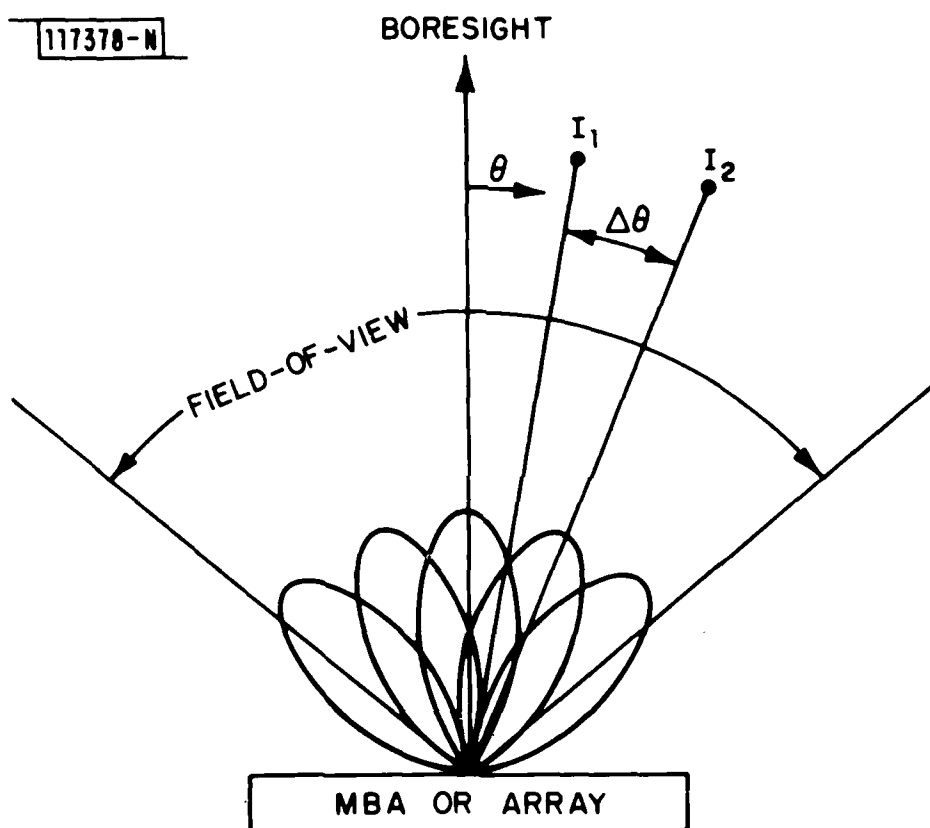


Fig. 1. Geometry for two interference sources (I_1 , I_2) in the field of view of either a multiple-beam antenna or a phased array antenna.

location of each element of either an adaptive phased array or multiple-beam antenna. That is, they are independent of scan angle because the channel covariance matrix is formed prior to weighting or beam forming.

A basic adaptive nulling system block diagram for N-channels is shown in Figure 2. The signals $S_1(t)$, $S_2(t)$, ..., $S_N(t)$ are received by either the feeds of an MBA or the elements of a phased array. These signals are coupled to the adaptive processor which performs the cross-correlation operation. The adaptive processor controls the weights w_1 , w_2 , ..., w_N such that the output signal $y(t)$ does not contain (ideally) any incident interference power.*

It is instructive to examine how the interference covariance matrix eigenvectors and eigenvalues are related to adaptive nulling. Typically, for a single strong interference source, the covariance matrix has one large eigenvalue (compared to the quiescent receiver noise level) and a corresponding eigenvector. Suppose that the interference signal is incident in the direction of the antenna's first sidelobe. The radiation pattern shown in Figure 3 is prior to adaption and is the pattern obtained for a uniformly illuminated 150-wavelength diameter circular aperture (i.e., $J_1(x)/x$).

The eigenvector corresponding to the single large eigenvalue of the interference covariance matrix can be considered as a weight vector. If this eigenvector is applied as a weight^[2], the pattern shown in Figure 4 results. The eigenvector weight creates a beam pointed at the interference

*It is assumed here that only interference signals are sensed by the processor. This means that desired incident signals have less power over the nulling bandwidth than the interference signals. This avoids the problem of nulling desired signals by mistake.

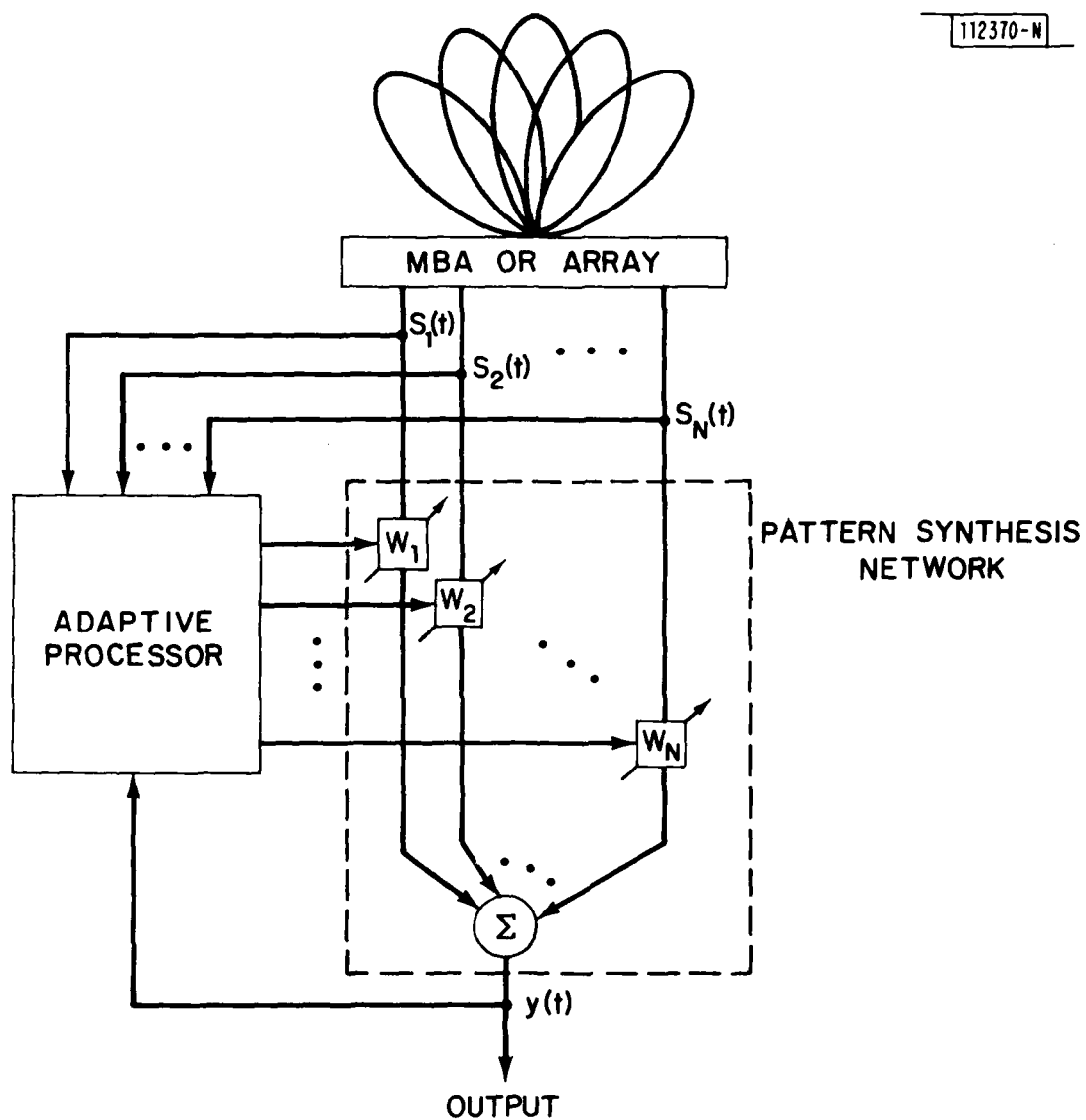


Fig. 2. Block diagram for an N-channel adaptive nulling system.

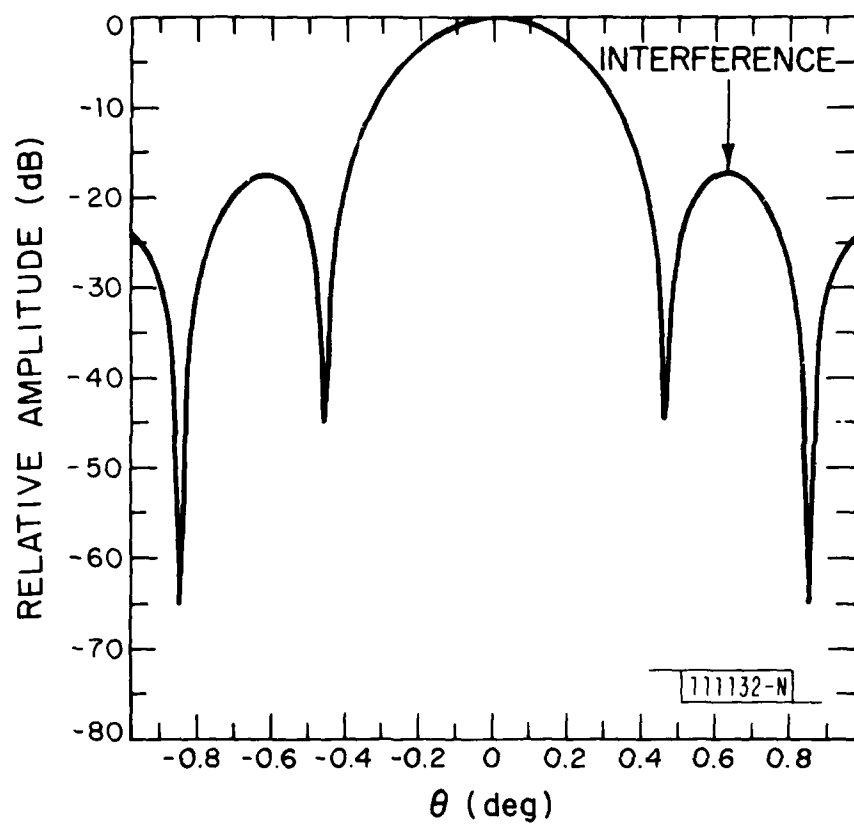


Fig. 3. Radiation pattern before adaption.

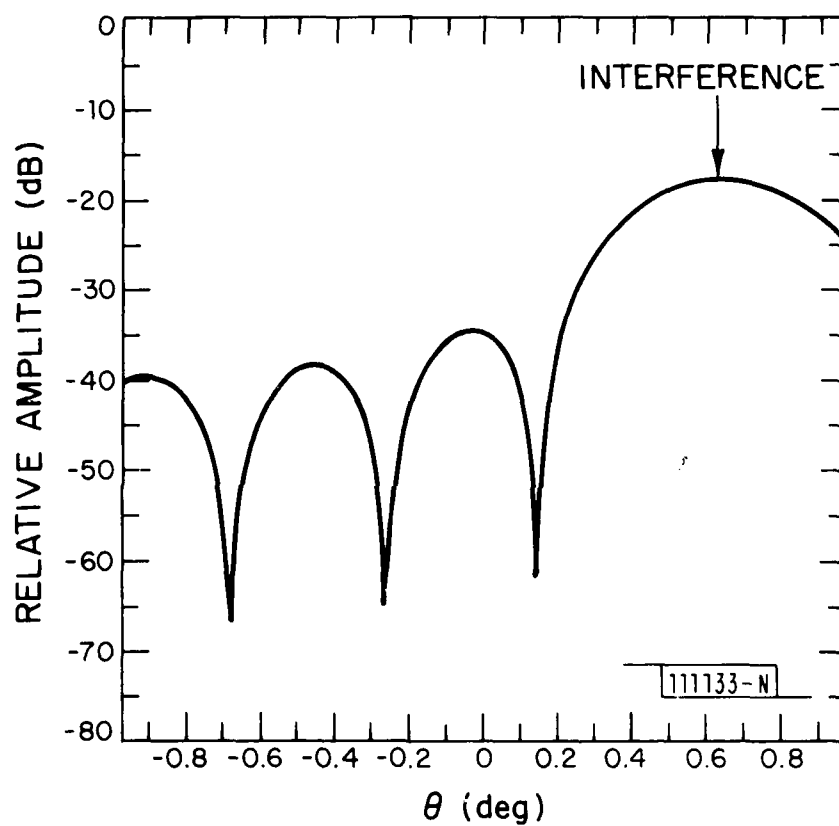


Fig. 4. Radiation pattern using the dominant eigenvector as a weight.

source. The beam amplitude is adjusted to the unadapted pattern sidelobe level at the interference source location. When the eigenvector radiation pattern is subtracted from the quiescent pattern, a null results at the interference location as shown in the adapted pattern in Figure 5.

Often the number of degrees of freedom used by an adaptive antenna in any given scenario is assumed to be equal to the number of interference sources nulled. This assumption is usually in error. The reason for this is suggested by the examples given in Figures 6 and 7. Figure 6 (contour plot) represents a communications link to a desired user at a known location in the antenna field of view. In this case, the antenna forms a maximum directivity beam in the user direction. If two interference sources (denoted by I_1 , I_2) are in the field of view, the antenna adaptively creates a null region* which, typically, intersects both sources. Since discrete (point) nulls are not created in this case, it is not possible, by inspection of the adapted radiation pattern, to count the number of degrees of freedom consumed.

A second case of interest is for uniform pattern coverage over the field of view. This corresponds to a communications link where the system users have unknown locations. In Figure 7, two interference sources are in the antenna field of view. Some typical examples of the shape of the null region formed for various source spacings are given. For close spacing (less than one half-power beamwidth), both sources are contained by a single circular-shaped null region. For a source spacing close to one half-power beamwidth,

*A null region here is taken to be an area where the radiation pattern amplitude is down by more than 30 dB from the main beam peak.

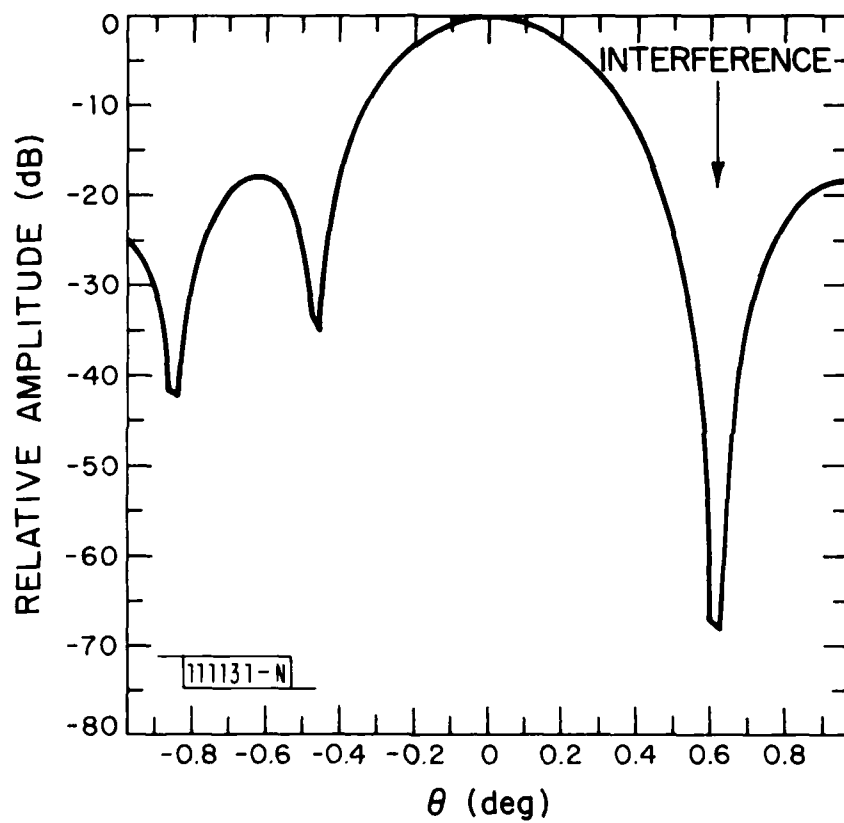


Fig. 5. Radiation pattern after adaption.

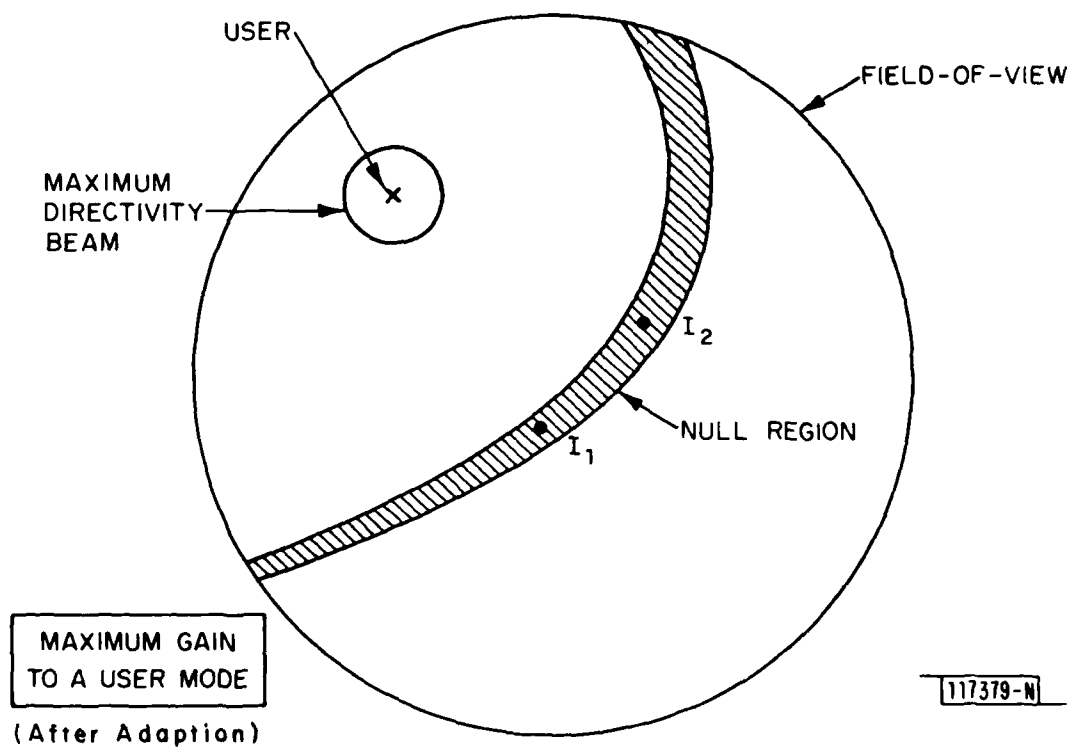
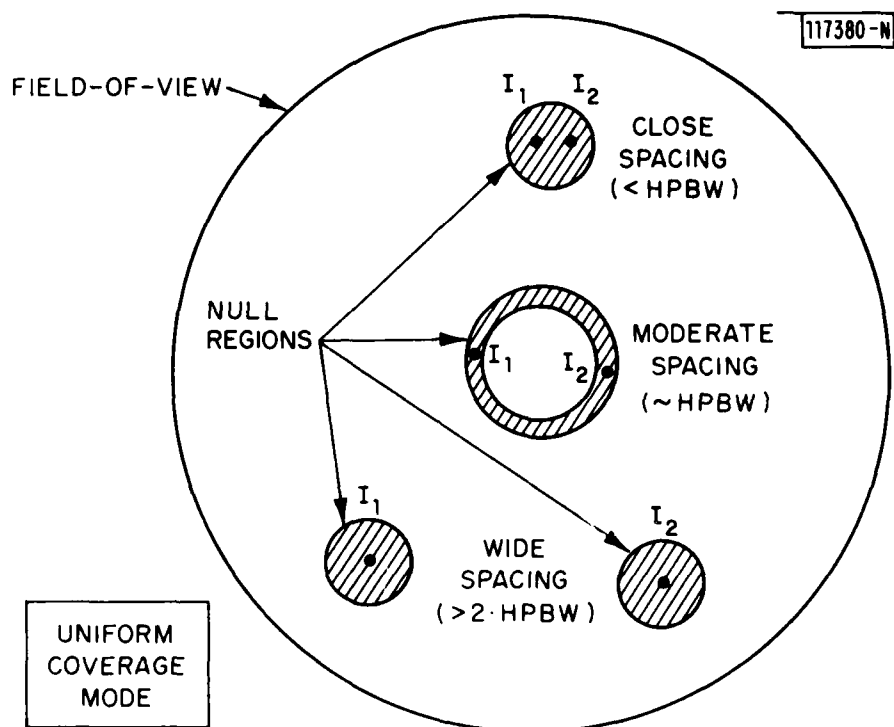


Fig. 6. Typical null-region shape for a communications link where the user is in a known location.



(After Adaption)

Fig. 7. Typical null-region shapes for various interference source spacings for a communications link where the users are in unknown locations.

the null region is ring shaped. When the sources are spaced greater than two half-power beamwidths apart, two separate circular-shaped null regions are formed. In the first case, it could be surmised that one degree of freedom is used to null two sources. Similarly, in the third case, it could be surmised that two degrees of freedom are consumed. However, for the second case, the number of degrees of freedom consumed is not clear.

From the above discussion, counting the interference sources which are nulled and setting this number equal to the degrees of freedom that are consumed can be misleading. A more general approach is to examine the eigenvalues of the interference covariance matrix. A count of the number of large eigenvalues present in the interference covariance matrix is a very accurate estimate of the degrees of freedom used. It is the intention of this paper to show how the eigenvalues vary as a function of the separation between two equal-power interference sources. This is investigated for a multiple-beam antenna and a phased array. The case of three or more interference sources is also addressed.

II. FORMULATION

A. Applebaum-Howells Analog Servo-Control-Loop Processor

The adaptive nulling algorithm used in this paper is the Applebaum-Howells analog servo-control-loop processor^[1,2,3]. For this algorithm the steady-state adapted antenna weight column vector is given by

$$\underline{w} = [\underline{I} + \mu \underline{R}]^{-1} \underline{w}_0 \quad (1)$$

where \underline{I} is the identity matrix

\underline{R} is the channel covariance matrix

μ is the effective loop gain which provides the threshold for sensing signals

\underline{w}_0 is a weight vector which gives a desired quiescent radiation pattern in the absence of interference sources.

For an N-channel adaptive nulling processor $[\underline{I} + \mu \underline{R}]$ is an NxN matrix. The covariance matrix elements are defined by

$$R_{pq} = \frac{1}{\omega_2 - \omega_1} \int_{\omega_1}^{\omega_2} S_p(\omega) S_q^*(\omega) d\omega \quad \begin{matrix} p = 1, 2, \dots, N \\ q = 1, 2, \dots, N \end{matrix} \quad (2)$$

where $\omega_2 - \omega_1$ is the nulling bandwidth

$S_p(\omega)$, $S_q(\omega)$ are the received voltages in the p^{th} and q^{th} channels, respectively, over the nulling bandwidth

* denotes complex conjugate.

B. Eigenvalues and Eigenvectors of the Interference Covariance Matrix

The covariance matrix defined by Eq. (2) is Hermitian (that is, $\underline{R} = \underline{R}^\dagger$ where \dagger means complex-conjugate-transposed) which by the spectral theorem can be decomposed in eigenspace as^[4]

$$\underline{R} = \sum_{k=1}^N \lambda_k \underline{e}_k \underline{e}_k^\dagger \quad (3)$$

where $\lambda_k, k=1,2,\dots,N$ are the eigenvalues of \underline{R}
 $\underline{e}_k, k=1,2,\dots,N$ are the eigenvectors of \underline{R} .

The matrix product $\underline{e}_k \underline{e}_k^\dagger$ is an $N \times N$ matrix which represents the projection onto eigenspace for λ_k . Comparing Eq. (2) and Eq. (3), it is observed that the eigenvalues have units of voltage squared, that is, the eigenvalues are proportional to power.

Substituting Eq. (3) into Eq. (1) and using the orthogonality property of the eigenvectors leads to the following expression for the adapted antenna weight vector. (Note: the complete derivation is given in the appendix.)

$$\underline{w} = \underline{w}_0 - \sum_{k=1}^N \frac{\mu \lambda_k}{1 + \mu \lambda_k} \langle \underline{e}_k^\dagger, \underline{w}_0 \rangle \underline{e}_k \quad (4)$$

where $\langle \underline{e}_k^\dagger, \underline{w}_0 \rangle = \underline{e}_k^\dagger \underline{w}_0$ is a complex scalar.

Each of the vectors in Eq. (4) are weights which can be applied to the adaptive antenna. From Eq. (4), and using the principle of superposition, the adapted far-field pattern can be written as

$$P(\theta, \phi; \underline{w}) = P_0(\theta, \phi; \underline{w}_0) - \sum_{k=1}^N \frac{\mu \lambda_k}{1 + \mu \lambda_k} \langle \underline{e}_k^\dagger, \underline{w}_0 \rangle P_k(\theta, \phi; \underline{e}_k) \quad (5)$$

where $P(\theta, \phi; \underline{w})$ is the adapted radiation pattern

$P_0(\theta, \phi; \underline{w}_0)$ is the quiescent radiation pattern

$P_k(\theta, \phi; \underline{e}_k)$ is the k^{th} eigenvector radiation pattern.

Eq. (5) shows how the quiescent radiation pattern is modified in the presence of interference sources. The scalar $\langle \underline{e}_k^\dagger, \underline{w}_0 \rangle$ is the projection of the k^{th} eigenvector onto the quiescent antenna weight vector. If, for example, a single interference source (which gives rise to a single eigenvalue, λ_1 , and eigenvector, \underline{e}_1) lies on a null of the quiescent pattern, then $\langle \underline{e}_1^\dagger, \underline{w}_0 \rangle = 0$. No adaption is necessary which means that $\underline{w} = \underline{w}_0$. However, if a source lies on a sidelobe of the quiescent pattern, the inner product of \underline{e}_1^\dagger with \underline{w}_0 will be non-zero (see Figures 3 and 4). This projection is weighted by the quantity $\mu \lambda_1 / (1 + \mu \lambda_1)$ and subtracted from \underline{w}_0 . For a large value of λ_1 corresponding to a strong interference source, the product $\mu \lambda_1$ is much greater than unity. This implies that $\mu \lambda_1 / (1 + \mu \lambda_1) \approx 1$. Similarly, a weak interference source which has $\mu \lambda_1$ much less than unity results in $\mu \lambda_1 / (1 + \mu \lambda_1) \approx 0$. If another source sufficiently separated (approximately one half-power beamwidth) from the first is added, a second large eigenvalue, λ_2 , will occur. Two terms ($k=1,2$) would then be significant in Eq. (5).

From these examples, it is clear that strong sources will cause a larger change in the quiescent weight vector than weak sources. Eq. (5) has been

shown to be dependent on both interference source location and power level. Basically, the quiescent radiation pattern is modified by removing any projections of interference source eigenvectors on \underline{w}_0 . This is the fundamental mechanism by which the antenna forms a null (or nulls) in the direction of the interference.

In the next section, the eigenvalues of the interference covariance matrix are used to describe the consumption of the degrees of freedom of adaptive antennas. Specific examples of multiple-beam and phased array antennas are given.

III. TWO INTERFERENCE SOURCES

A. Multiple-Beam Antenna

A nineteen-beam MBA was chosen for a demonstration of the eigenvalue spread (denoted by $\Delta\lambda$) as a function of the angular separation between two interference sources. The MBA beams are located in a hexagonal grid which is shown in Figure 8. The antenna diameter was chosen to be $D=150\lambda$. With uniform aperture illumination the half-power beamwidth of each beam of the MBA is 0.39° ; the composite pattern of all nineteen beams results in a 2° diameter coverage area.

Standard spherical coordinates are used to represent a far-field point at (θ, ϕ) , where θ is the angle measured from boresight and ϕ is the azimuth angle about boresight. Two equal-power interference sources (I_1, I_2) are assumed to be located within the 2° coverage area. Source I_1 was chosen to be fixed at the half-power point of the center beam ($\theta=0.195^\circ, \phi=0^\circ$). Source I_2 was allowed to vary in angle from boresight, beginning with $\theta=0.195^\circ$ for ϕ fixed at 0° . The nulling bandwidth was assumed to be narrow in order to minimize the effects of bandwidth on the results. Thus, there are only two eigenvalues different from quiescent receiver noise in this case. The two eigenvalues, λ_1 for source I_1 and λ_2 for source I_2 , are displayed in Figure 9 as a function of source separation angle $\Delta\theta$. When the two sources are at the same location ($\Delta\theta=0^\circ$), only one large eigenvalue appears (one degree of freedom is used) which is 3 dB higher than for a single source. As the second source moves away from the first, its associated eigenvalue (λ_2) rises from 0 dB and is nearly equal to λ_1 ($\Delta\lambda=1.7$ dB) when the separation angle is equal to the half-

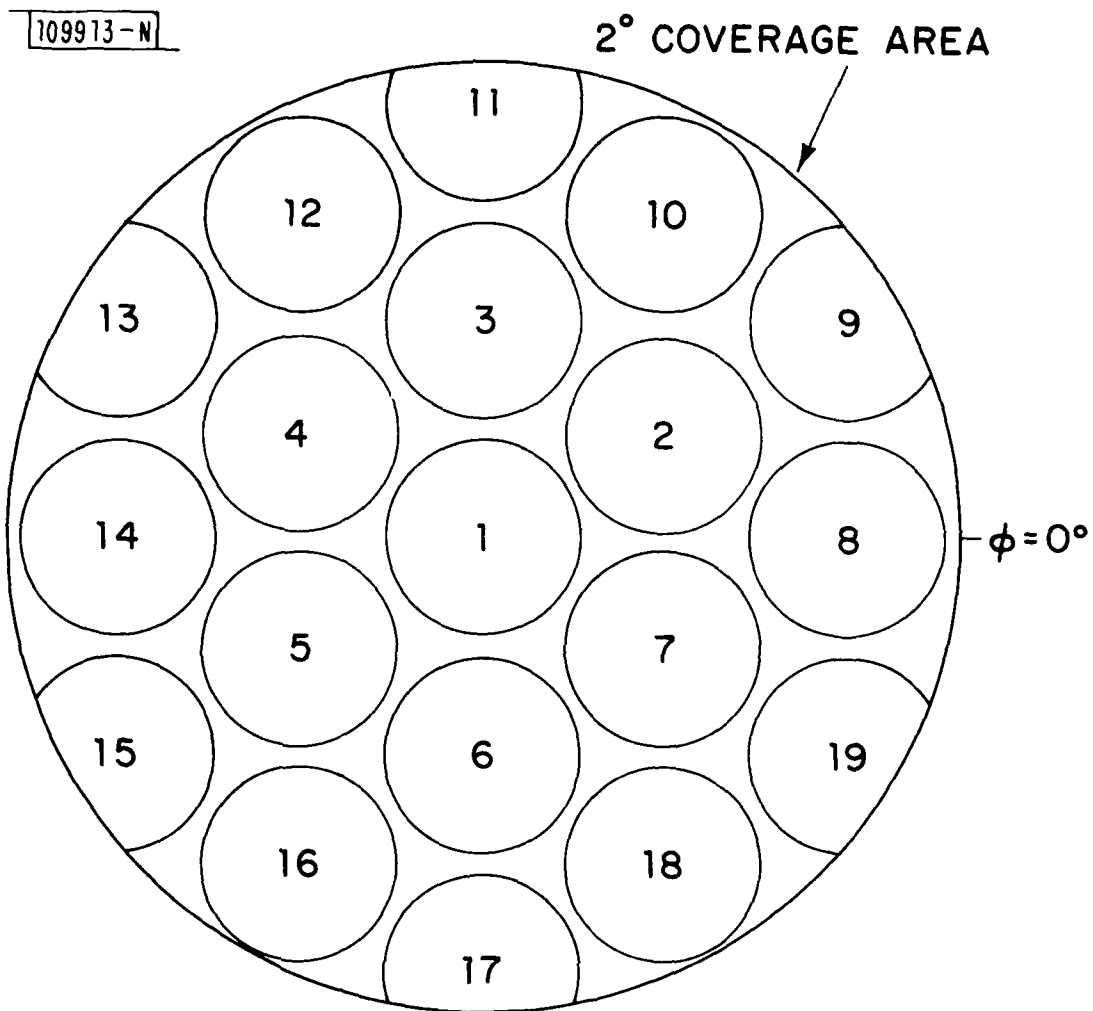


Fig. 8. Hexagonal beam positions for a 19-beam MBA.

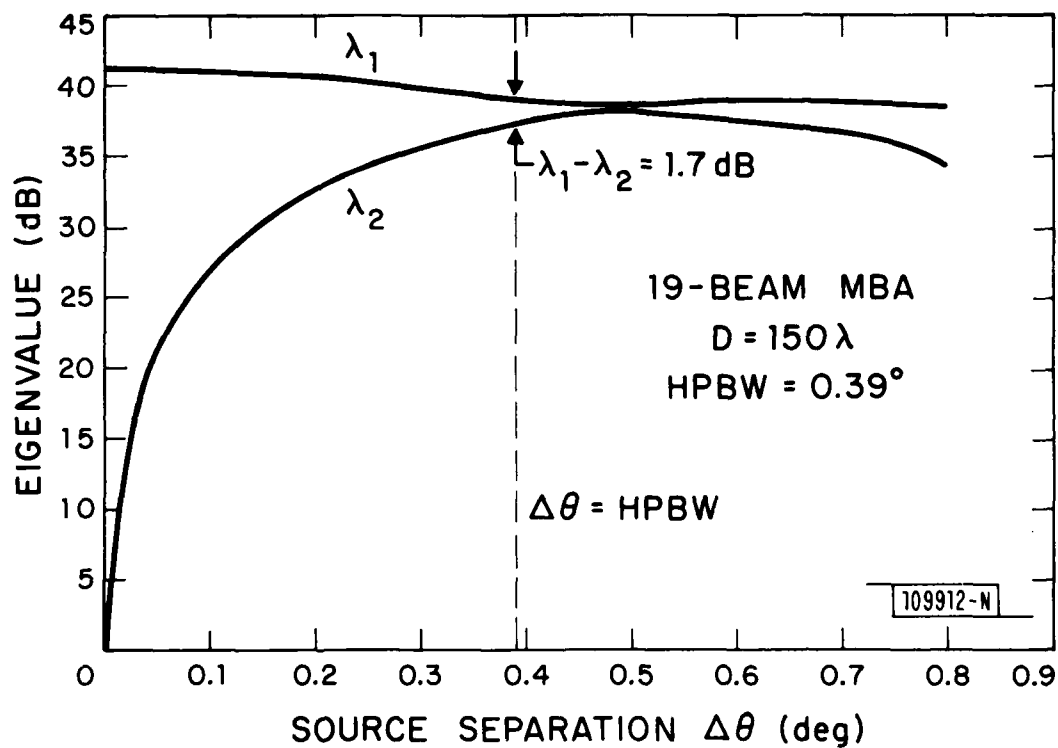


Fig. 9. Eigenvalue spread as a function of the separation between two interference sources in the field of view of a 19-beam MBA.

power beamwidth of the antenna. (The spread for separations greater than one half-power beamwidth decreases only slightly.) As is expected, λ_1 decreases slowly (by 3 dB) as the sources separate since source I_1 begins to behave as a single source. Additionally, source I_2 was varied in position on a circle with a radius equal to one half-power beamwidth and centered at source I_1 . It was found that the eigenvalue spread ($\lambda_1 - \lambda_2$) is between 1.6 dB to 2.0 dB for twelve positions spaced uniformly about the circle.

The above results suggest that a source separation of approximately one-half power beamwidth or larger is required to cause the MBA to use two degrees of freedom. This occurs when the two dominant eigenvalues are large and are approximately equal. In the following section it is shown that the same criterion applies to an adaptive array.

B. Phased Array Antenna

A ten-element uniform circular ring array was chosen for demonstrating the eigenvalue spread as a function of the spacing between two interference sources in the field of view of a thinned phased array. As for the MBA example, the array diameter was chosen to be $D=150\lambda$, and the coverage area was again chosen to be two degrees in diameter. The array elements have a half-power beamwidth that subtends this 2° diameter coverage area. This array configuration, with the array elements located on the circumference of the circle, shown in Figure 10, has the highest resolution (narrowest beamwidth) for a given planar aperture size^[5]. With all array elements excited equally, the ring array half-power beamwidth (HPBW) is related to the aperture diameter by $\text{HPBW} \cong 0.72\lambda/D$ radians. The half-power beamwidth for the present example is 0.274° .

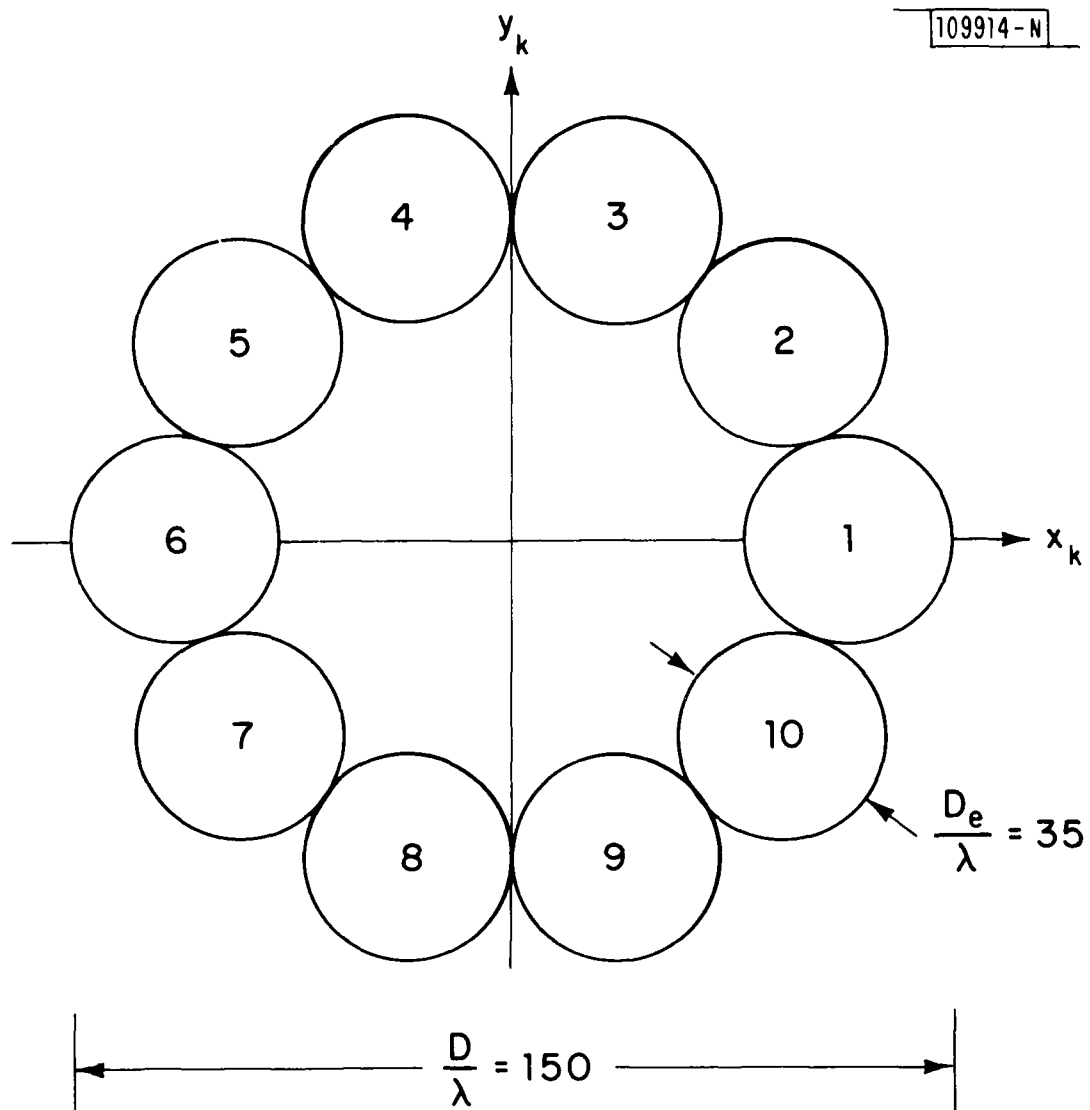


Fig. 10. A ten-element circular ring array designed for a 2° coverage area.

As was done in the MBA example, two interference sources (I_1, I_2) are assumed to lie within the 2° coverage area. Source I_1 is fixed at the half-power point ($\theta=0.137^\circ, \phi=0^\circ$) of the main beam in the boresight position. Source I_2 varies in position from $\theta=0.137^\circ$ (positive increments) for with ϕ fixed at 0° . There are only two eigenvalues (λ_1, λ_2) different from quiescent noise (again, with narrowband nulling) in this case. These are plotted in Figure 11 as a function of the source separation $\Delta\theta$. This behavior is very similar to that shown for the MBA. Eigenvalue λ_1 is reduced in power by approximately 3 dB as the sources separate beyond one half-power beamwidth. A minimum eigenvalue spread (approximately 0.7 dB) occurs at approximately one half-power beamwidth separation. Next, source I_2 was moved uniformly for twelve positions on a circle with a half-power beamwidth radius centered at source I_1 . The eigenvalue value spread ($\lambda_1-\lambda_2$) was found to be between 0.2 dB and 0.5 dB. Thus, like the MBA, two interference sources separated by one half-power beamwidth or more use two degrees of freedom.

In the next section the eigenvalue spread for three interference sources is examined. A discussion of the case where there are as many interference sources as there are degrees of freedom then follows.

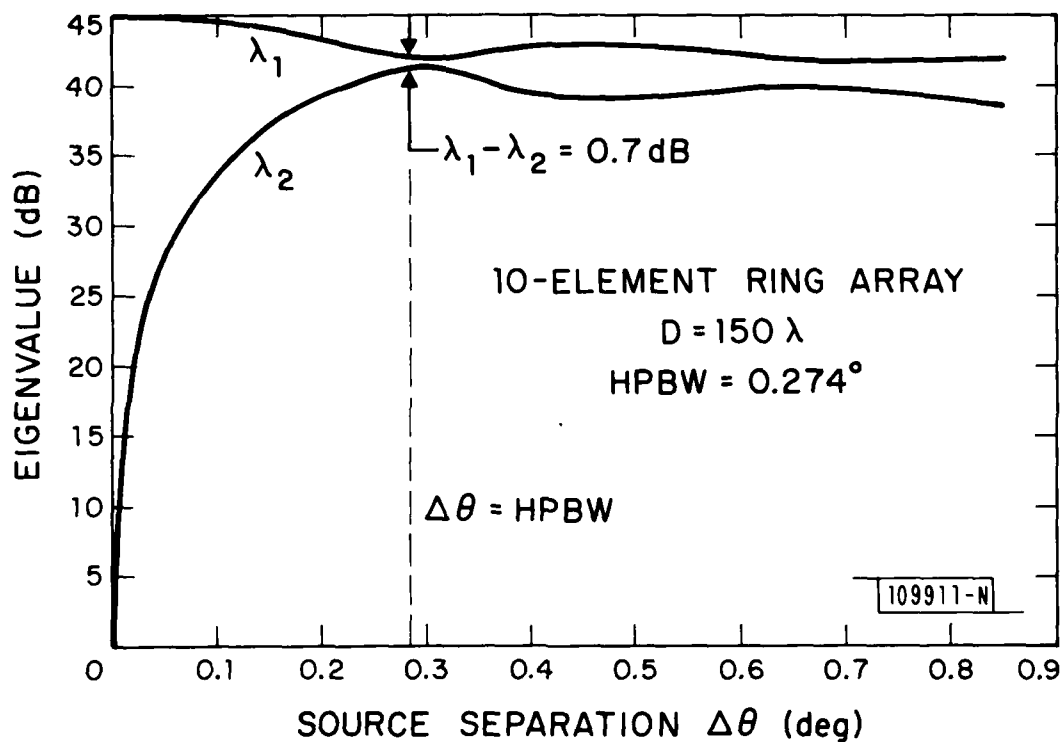


Fig. 11. Eigenvalue spread as a function of the separation between two interference sources in the field of view of a ten-element circular ring array.

IV. THREE INTERFERENCE SOURCES

A. MBA and Array Results

With two interference sources in the field of view of an adaptive antenna, the previous section shows that each source consumes one degree of freedom when the separation between sources is approximately equal to or greater than the antenna half-power beamwidth. This section examines two simple configurations of three equal-power sources, one is a straight line (constant azimuth angle), the other an equilateral triangle. In each configuration, the sources are separated by one half-power beamwidth.

First, consider the 19-beam MBA shown in Figure 8. For three sources on a straight line ($\theta=0.195^\circ, 0.585^\circ, 0.975^\circ$; $\phi=0^\circ$) the three eigenvalues are computed to be $\lambda_1=39.1$ dB, $\lambda_2=38.2$ dB, and $\lambda_3=32.1$ dB. This is a spread of 7.0 dB which indicates that three degrees of freedom are not completely used. However, with three sources on an equilateral triangle (each side equal to one half-power beamwidth), the eigenvalues are found to be $\lambda_1=39.7$ dB, $\lambda_2=37.2$ dB, $\lambda_3=37.1$ dB. The spread is 2.6 dB which suggests that three degrees of freedom have been nearly completely used.

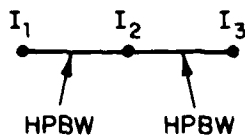
The ten-element array (see Figure 10) shows a somewhat different behavior from the MBA. For three sources on a straight line ($\theta=0.137^\circ, 0.411^\circ, 0.685^\circ$; $\phi=0^\circ$) the three eigenvalues are computed to be $\lambda_1=42.4$ dB, $\lambda_2=41.4$ dB, and $\lambda_3=39.1$ dB. The spread is 3.3 dB which implies that three degrees of freedom are almost fully used (this was not true for the MBA.). With an equilateral triangle configuration, the eigenvalues are $\lambda_1=41.7$ dB, $\lambda_2=41.3$ dB, and $\lambda_3=41.1$ dB, which is a spread of only 0.6 dB. Again, three degrees of freedom

are being used. (The above results are summarized in Table 1.) Complete consumption of three degrees of freedom occurs when the three dominant eigenvalues computed from the interference covariance matrix are equal.

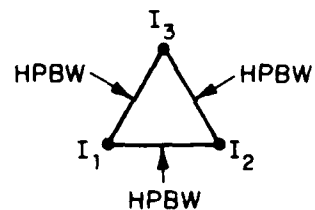
From these examples it is observed that the equilateral-triangle source configuration causes an adaptive antenna (two-dimensional) to use its degrees of freedom more completely than for three sources on a straight line. For a straight-line configuration, three sources consumed three degrees of freedom more completely for the 10-element array than they did for the 19-beam MBA. In other words, consumption of degrees of freedom is dependent on the interference source configuration and the antenna geometry.

TABLE 1
A SUMMARY OF THE EIGENVALUE SPREAD FOR TWO CONFIGURATIONS OF THREE
INTERFERENCE SOURCES IN THE FIELD OF VIEW OF AN ARRAY AND AN MBA

STRAIGHT LINE



EQUILATERAL TRIANGLE



ANTENNA TYPE	INTERFERENCE TYPE	EIGENVALUE SPREAD
MBA 19 BEAMS (Hexagonal)	STRAIGHT LINE EQUILATERAL TRIANGLE	$\Delta\lambda = 7.0$ dB $\Delta\lambda = 2.6$ dB *
PHASED ARRAY 10-ELEMENTS (Circular-Ring)	STRAIGHT LINE EQUILATERAL TRIANGLE	$\Delta\lambda = 3.3$ dB $\Delta\lambda = 0.6$ dB *

* THREE DEGREES OF FREEDOM ARE CONSUMED

V. DISCUSSION AND CONCLUSIONS

The goal of this paper is to illustrate quantitatively the utilization of adaptive antenna degrees of freedom when interference sources are present. This is done by relating the eigenvalue spread to the spacing of the interference sources. It is shown that when two interference sources are spaced less than one-half power beamwidth apart, the covariance matrix possesses only one dominant eigenvalue, indicating that only one degree of freedom is required to null both sources. As the source spacing approaches one half-power beamwidth, a second eigenvalue approximately equal to the first occurs. Thus, for the case of two interference sources, a source spacing equal to one half-power beamwidth or more is required to cause the antenna to fully utilize two degrees of freedom to null the interference. With three interference sources, an equilateral triangle configuration (with one half-power beamwidth spacing) caused both the array and the MBA to use three degrees of freedom more completely than did a straight line configuration. A basic conclusion of this study is that the amount by which the degrees of freedom are consumed depends on both the interference source configuration and the antenna geometry.

A scenario of interest is the placement of N interference sources in the field of view of an N -channel adaptive antenna, such that $N-1$ degrees of freedom are consumed by $N-1$ of the sources, and the N^{th} source jams the system by capturing the last remaining degree of freedom. From the previous discussion one might conclude that the eigenvalue spread among the N eigenvalues should be less than 3 dB to insure consumption of N -degrees of freedom. Based on the results given for two and three sources, a minimum

necessary condition to achieve this is to separate the sources such that no two are less than one half-power beamwidth apart. However, the antenna beams represented by the eigenvectors can have complicated patterns when many sources are present (e.g., bifurcated beams), so this approach will not necessarily be successful. The exact configuration of the interference sources depends on the antenna geometry, particularly the half-power beamwidth. It is expected that in some situations, N interference sources may not be adequate to completely consume N -degrees of freedom. A detailed study will be necessary to determine the susceptibility to interference for a specific antenna type.

APPENDIX A

DERIVATION OF THE APPLEBAUM-HOWELLS STEADY STATE ADAPTED WEIGHT EQUATION IN EIGENSPACE

In this appendix, Eq. (4) is derived which relates the adapted weight vector to the eigenvalues and eigenvectors of the interference covariance matrix. Based on the Applebaum-Howells analog servo-control-loop processor, the steady state adapted weight column vector^[1,2,3] (denoted by \underline{w}) is

$$\underline{w} = [\underline{I} + \mu \underline{R}]^{-1} \underline{w}_0 \quad (\text{A-1})$$

where \underline{I} is the identity matrix

\underline{R} is the channel covariance matrix

μ is the effective loop gain which provides the threshold for sensing signals

\underline{w}_0 is a weight vector which gives a desired quiescent radiation pattern in the absence of interference sources.

For an N-channel adaptive nulling processor $[\underline{I} + \mu \underline{R}]$ is an NxN matrix. It is useful to relate \underline{w} to the eigenvalues λ_k and eigenvectors \underline{e}_k of \underline{R} such that

$$\underline{R} \cdot \underline{e}_k = \lambda_k \underline{e}_k, \quad k = 1, 2, \dots, N \quad (\text{A-2})$$

The covariance matrix elements are defined to be

$$R_{pq} = \frac{1}{\omega_2 - \omega_1} \int_{\omega_1}^{\omega_2} S_p(\omega) S_q^*(\omega) d\omega \quad \begin{matrix} p=1,2,\dots,N \\ q=1,2,\dots,N \end{matrix} \quad (A-3)$$

where $\omega_2 - \omega_1$ is the nulling bandwidth

$S_p(\omega)$, $S_q(\omega)$ are the received voltages in the p^{th} and q^{th} channels, respectively, over the nulling bandwidth

* denotes complex conjugate.

Noting that $R_{p,q} = R_{q,p}^*$ in Eq. (A-3) \underline{R} is recognized as a Hermitian matrix. According to the spectral theorem^[3] a Hermitian matrix such as \underline{R} , can be decomposed in eigenspace as

$$\underline{R} = \sum_{k=1}^N \lambda_k \underline{P}_k \quad (A-4a)$$

where $\underline{P}_k = \underline{e}_k \underline{e}_k^\dagger$ is the k^{th} projection matrix (note: the superscript \dagger means complex conjugate-transpose). That is, \underline{P}_k is the projection onto the eigenspace for λ_k and

$$\sum_{k=1}^N \underline{P}_k = \underline{I} \quad .$$

The concept of a projection matrix will be made somewhat clearer by the discussion following Eq. (A-6).

It is useful to compare Eqs. (A-3) and (A-4a) and observe that the eigenvalues are proportional to power. Note: an equivalent expression for the covariance matrix is

$$\underline{\underline{R}} = \underline{\underline{Q}} \underline{\underline{\Lambda}} \underline{\underline{Q}}^{\dagger} \quad (\text{A-4b})$$

where $\underline{\underline{Q}}$ is a transformation matrix whose columns are the eigenvectors of $\underline{\underline{R}}$,

$$\underline{\underline{\Lambda}} = \text{diag} [\lambda_1, \lambda_2, \dots, \lambda_n] .$$

By matrix multiplication, it can be shown that

$$\underline{\underline{Q}} \underline{\underline{\Lambda}} \underline{\underline{Q}}^{\dagger} = \sum_{k=1}^N \lambda_k \underline{\underline{e}}_k \underline{\underline{e}}_k^{\dagger} .$$

Using Eq. (A-4a), Eq. (A-1) can now be written as

$$[\underline{\underline{I}} + \mu \sum_{k=1}^N \lambda_k \underline{\underline{e}}_k \underline{\underline{e}}_k^{\dagger}] \underline{\underline{w}} = \underline{\underline{w}}_0 \quad (\text{A-5})$$

or

$$\underline{\underline{w}} + \mu \sum_{k=1}^N \lambda_k \underline{\underline{e}}_k \langle \underline{\underline{e}}_k^{\dagger}, \underline{\underline{w}} \rangle = \underline{\underline{w}}_0 \quad (\text{A-6})$$

where $\langle \underline{\underline{e}}_k^{\dagger}, \underline{\underline{w}}_0 \rangle = \underline{\underline{e}}_k^{\dagger} \underline{\underline{w}}_0$ is a complex scalar. Note that in the summation in Eq. (A-6), the adapted weight vector $\underline{\underline{w}}$ has been projected onto the k^{th} eigenvector $\underline{\underline{e}}_k$. This projection is weighted by λ_k which is then reassembled

to form the matrix product $R\bar{w}$. Next, take the product of $\underline{e}_\ell^\dagger$, $\ell=1,2,\dots,N$ with Eq. (A-6) which yields

$$\langle \underline{e}_\ell^\dagger, \bar{w} \rangle + \mu \sum_{k=1}^N \lambda_k \langle \underline{e}_\ell^\dagger, \underline{e}_{-k} \rangle \langle \underline{e}_{-k}^\dagger, \bar{w} \rangle = \langle \underline{e}_\ell^\dagger, \bar{w}_0 \rangle, \quad \ell=1,2,\dots,N. \quad (\text{A-7})$$

The eigenvectors are, by definition, orthogonal, which implies that

$$\langle \underline{e}_\ell^\dagger, \underline{e}_k \rangle = \begin{cases} 1 & \text{if } k = \ell \\ 0 & \text{if } k \neq \ell \end{cases} \quad (\text{A-8})$$

from which it follows that

$$\langle \underline{e}_\ell^\dagger, \bar{w} \rangle + \mu \lambda_\ell \langle \underline{e}_\ell^\dagger, \bar{w} \rangle = \langle \underline{e}_\ell^\dagger, \bar{w}_0 \rangle \quad \ell=1,2,\dots,N. \quad (\text{A-9})$$

Factoring $\langle \underline{e}_\ell^\dagger, \bar{w} \rangle$ on the left side of Eq. (A-9) and substituting k for ℓ yields

$$\langle \underline{e}_k^\dagger, \bar{w} \rangle = \frac{\langle \underline{e}_k^\dagger, \bar{w}_0 \rangle}{1 + \mu \lambda_k} \quad k=1,2,\dots,N. \quad (\text{A-10})$$

Substituting Eq. (A-10) into Eq. (A-6) gives the result for the adapted weight vector

$$\underline{w} = \underline{w}_0 - \sum_{k=1}^N \frac{\mu\lambda_k}{1+\mu\lambda_k} \langle \underline{e}_k^\dagger, \underline{w}_0 \rangle \underline{e}_k \quad (A-11)$$

Equation (A-11) shows how the quiescent weight vector is modified in the presence of interference sources. The scalar $\langle \underline{e}_k^\dagger, \underline{w}_0 \rangle$ is the projection of the eigenvector \underline{e}_k on the quiescent weight vector. For values of $\mu\lambda_k < 1$, corresponding to weak interference sources, the adapted weight vector is relatively unchanged from \underline{w}_0 . However, when the interference sources are strong, the eigenvalues are large ($\mu\lambda_k > 1$), and the adapted weight vector tends to be more strongly varied from \underline{w}_0 . This is due to the influence of the $(\mu\lambda_k / 1 + \mu\lambda_k) \langle \underline{e}_k^\dagger, \underline{w}_0 \rangle$ factor. The negative summation essentially removes any projections of interference source eigenvectors from the quiescent weight vector, which causes the adapted antenna pattern to have a null in the direction of the interference.

Equation (A-11) can be expressed in another useful form by observing that \underline{w}_0 can be written as

$$\underline{w}_0 = \sum_{\ell=1}^N \gamma_\ell \underline{e}_\ell \quad (A-12)$$

where the γ_ℓ are appropriately chosen constants. This is true, because the eigenvectors make up a complete orthogonal set of vectors, so any vector such as \underline{w}_0 can be decomposed into a sum of appropriately weighted eigenvectors. To evaluate γ_ℓ , take the scalar product of \underline{e}_k^\dagger with Eq. (A-12). This yields

$$\langle \underline{e}_{-k}^\dagger, \underline{w}_{-0} \rangle = \sum_{\ell=1}^N \gamma_{\ell} \langle \underline{e}_{-k}^\dagger, \underline{e}_{-\ell} \rangle \quad k=1,2,\dots,N \quad . \quad (\text{A-13})$$

By the orthogonality property it is clear that

$$\langle \underline{e}_{-\ell}^\dagger, \underline{w}_{-0} \rangle = \gamma_{\ell} \quad , \quad \text{hence}$$

$$\underline{w}_{-0} = \sum_{\ell=1}^N \langle \underline{e}_{-\ell}^\dagger, \underline{w}_{-0} \rangle \underline{e}_{-\ell} \quad (\text{A-14})$$

Substituting Eq. (A-14) into Eq. (A-11) yields

$$\underline{w} = \sum_{\ell=1}^N \langle \underline{e}_{-\ell}^\dagger, \underline{w}_{-0} \rangle \underline{e}_{\ell} - \sum_{k=1}^N \frac{\mu \lambda_k}{1 + \mu \lambda_k} \sum_{\ell=1}^N \langle \underline{e}_{-\ell}^\dagger, \underline{w}_{-0} \rangle \langle \underline{e}_{-k}^\dagger, \underline{e}_{\ell} \rangle \underline{e}_k \quad (\text{A-15})$$

Making use of orthogonality (Eq. A-8) in Eq. (A-15) gives

$$\underline{w} = \sum_{\ell=1}^N \langle \underline{e}_{-\ell}^\dagger, \underline{w}_{-0} \rangle \underline{e}_{\ell} - \sum_{\ell=1}^N \frac{\mu \lambda_{\ell}}{1 + \mu \lambda_{\ell}} \langle \underline{e}_{-\ell}^\dagger, \underline{w}_{-0} \rangle \underline{e}_{\ell} \quad (\text{A-16})$$

which reduces to

$$\underline{w} = \sum_{\ell=1}^N \frac{1}{1 + \mu \lambda_{\ell}} \langle \underline{e}_{-\ell}^\dagger, \underline{w}_{-0} \rangle \underline{e}_{\ell} \quad . \quad (\text{A-17})$$

Equation (A-17) is the same result given by Mayhan^[13]. In this equation, eigenvectors corresponding to large eigenvalues do not contribute significantly to the adapted weight \underline{w} . This assures that strong interference sources will be effectively nulled.

REFERENCES

1. J. T. Mayhan, A. J. Simmons, and W. C. Cummings, "Wide-band Adaptive Antenna Nulling Using Tapped Delay Lines," IEEE Trans. Antennas Propag. AP-29, 923 (1981).
2. W. F. Gabriel, "An Introduction to Adaptive Arrays," Proc. IEEE, 64, 239 (1976).
3. J. T. Mayhan, "Some Techniques for Evaluating the Bandwidth Characteristics of Adaptive Nulling Systems," IEEE Trans. Antennas Propag. AP-27, 363 (1979).
4. G. Strang, Linear Algebra and Its Applications, (Academic Press, Inc., New York, NY, 1976).
5. J. T. Mayhan, "Thinned Array Configurations for Use with Satellite-Based Adaptive Antennas," IEEE Trans. Antennas Propag. AP-28, 846 (1980).

ACKNOWLEDGMENTS

The author is grateful to Mr. William C. Cummings, Dr. Alan J. Simmons, and Dr. Leon J. Ricardi for their contributions to this study.

UNCLASSIFIED

SECURITY CLASSIFICATION OF THIS PAGE (When Data Entered)

REPORT DOCUMENTATION PAGE		READ INSTRUCTIONS BEFORE COMPLETING FORM
1. REPORT NUMBER ESD-TR-82-047	2. GOVT ACCESSION NO. AD-A116588	3. RECIPIENT'S CATALOG NUMBER
4. TITLE (and Subtitle) Interference Sources and Degrees of Freedom in Adaptive Nulling Antennas		5. TYPE OF REPORT & PERIOD COVERED Technical Report
		6. PERFORMING ORG. REPORT NUMBER Technical Report 604 ✓
7. AUTHOR(s) Alan J. Fenn		8. CONTRACT OR GRANT NUMBER(s) F19628-80-C-0002
9. PERFORMING ORGANIZATION NAME AND ADDRESS Lincoln Laboratory, M.I.T. P.O. Box 73 Lexington, MA 02173-0073		10. PROGRAM ELEMENT, PROJECT, TASK AREA & WORK UNIT NUMBERS Program Element No. 33126K
11. CONTROLLING OFFICE NAME AND ADDRESS Defense Communications Agency 8th Street and So. Courthouse Road Arlington, VA 22204		12. REPORT DATE 12 May 1982
14. MONITORING AGENCY NAME & ADDRESS (if different from Controlling Office) Electronic Systems Division Hanscom AFB, MA 01731		13. NUMBER OF PAGES 42
		15. SECURITY CLASS. (of this report) Unclassified
15a. DECLASSIFICATION DOWNGRADING SCHEDULE		
16. DISTRIBUTION STATEMENT (of this Report) Approved for public release; distribution unlimited.		
17. DISTRIBUTION STATEMENT (of the abstract entered in Block 20, if different from Report)		
18. SUPPLEMENTARY NOTES None		
19. KEY WORDS (Continue on reverse side if necessary and identify by block number) interference sources multiple-beam antenna adaptive nulling phased array antenna		
20. ABSTRACT (Continue on reverse side if necessary and identify by block number) It is sometimes desirable to know how many interference sources an N-element phased array or N-beam multiple-beam antenna can adaptively null. This problem is usually addressed by considering the antenna to have at most N-1 degrees of freedom available for placing nulls on interference sources. However, if some of the N-1 sources are very close together, it is possible that less than N-1 degrees of freedom are used. This paper quantitatively describes this effect by examining the eigenvalue spread of the interference covariance matrix. It is shown in the case of two equal-power interference sources in the field of view of either a multiple-beam antenna, or a phased array antenna, the two dominant eigenvalues are approximately equal when the source separation is equal to one half-power beamwidth. In other words, two degrees of freedom are consumed by two interference sources then they are separated by approximately one half-power beamwidth. This effect is also investigated for several configurations of three interference sources. To consume three degrees of freedom, it is shown that the eigenvalue spread is dependent on the interference source configuration and the antenna geometry.		

UNCLASSIFIED

SECURITY CLASSIFICATION OF THIS PAGE (When Data Entered)